The Interpretation of Current-Clamp Recordings in the Cell-Attached Patch-Clamp Configuration

M. J. Mason, A. K. Simpson, M. P. Mahaut-Smith, and H. P. C. Robinson
Department of Physiology, University of Cambridge, United Kingdom

ABSTRACT In these experiments we have investigated the feasibility and accuracy of recording steady-state and dynamic changes in transmembrane potential noninvasively across an intact cell-attached patch using the current-clamp mode of a conventional patch-clamp amplifier. Using an equivalent circuit mimicking simultaneous whole-cell voltage-clamp and cell-attached current-clamp recordings we have defined both mathematically and experimentally the relationship between the membrane patch resistance, the seal resistance, and the fraction of the whole-cell potential recorded across an intact membrane patch. This analysis revealed a steep increase in the accuracy of recording of steady-state membrane potential as the seal/membrane ratio increases from 0. The recording accuracy approaches 100% as the seal/membrane ratio approaches infinity. Membrane potential measurements across intact cell-attached patches in rat basophilic leukemia cells and rat megakaryocytes revealed a surprisingly high degree of accuracy and demonstrated the ability of this noninvasive technique to follow dynamic changes in potential in nonexcitable cells.

INTRODUCTION

The potential difference across the plasma membrane plays a key role in controlling function in all cell types. As a result, measurements of membrane potential, both steady-state and dynamic changes, have become key to understanding the activation and regulation of cellular responses. Both invasive and noninvasive methods exist for the measurement of membrane potential. Sharp electrode, intracellular microelectrode recordings using voltage-follower amplifiers are firmly established and have provided important information about both steady-state and rapid biological changes in potential. However, this invasive approach has its drawbacks. The mere fact that the cell must be impaled with a microelectrode containing an electrolyte solution that is not identical to the ionic constituents of the cytosol are two causes for concern. Additionally, the use of intracellular recordings of this type is limited to large cells. This limitation of cell size in intracellular recording of membrane potential has been partially overcome by the use of current-clamp recording using the whole-cell mode of the patch-clamp technique in the tight seal configuration (Neher and Sakmann, 1978; Hamill et al., 1981). The composition of the pipette solution is more critical in the whole-cell patch-clamp configuration than with sharp electrodes since patch electrodes are of lower resistance, resulting in dialysis of the cytosol by the composition of the patch pipette (Pusch and Neher, 1988). This is a particularly important issue since dialysis can result in the loss of important cytosolic constituents including soluble kinases and phosphatases and small-molecular weight proteins and substrates required for the normal cellular functions setting membrane potential. This problem has been overcome by the use of the perforated patch technique (Horn and Marty, 1988; Rae et al., 1991). Nystatin and amphotericin have been used to reduce patch resistance for the purpose of obtaining adequate voltage control of the cell under voltage clamp and accurate measurements of membrane potential under current clamp without washing out large-molecular weight compounds. However, these agents reduce access resistance by introducing exogenous channels with high permeability, thus requiring careful consideration of the ionic composition of the patch pipette and the impact of this ionic composition on membrane potential.

Noninvasive techniques for the measurement of membrane potential have been used in a variety of cell types. The Nernstian distribution of radiolabeled compounds has been used to estimate transmembrane potential. Although this technique is of limited value for the measurement of dynamic changes in potential, given the requirement of steady-state isotope distribution for calibration of potential, it has proved useful for estimates of steady-state potential (Catterall et al., 1976; Lichtshtein et al., 1979).

A variety of potentiometric fluorescent indicators have been employed to monitor membrane potential in a variety of cellular preparations (Waggoner, 1979; Rink et al., 1980; Grinstein et al., 1984; Ehrenberg et al.,1988; London et al., 1989; Zhang et al., 1998; Orbach et al., 1985; Mason and Grinstein, 1990; Rohr and Salzberg, 1994; Mason et al.,1999; Kao et al., 2001). Although potentiometric indicators are noninvasive, the influence of the fluorescent probe on cellular function must be considered (Simons, 1979; Montecucco et al., 1979; Rink et al., 1980). An additional concern with potentiometric indicators is converting their fluorescence or absorbance recordings into meaningful measurements of potential.

Submitted July 16, 2004, and accepted for publication October 19, 2004.

Address reprint requests to Dr. Michael J. Mason, Dept. of Physiology, University of Cambridge, Downing St., Cambridge CB2 3EG, UK. Tel.: 44-1223-333899; E-mail: mjm39@cam.ac.uk.

0006-3495/05/01/739/12 $2.00

doi: 10.1529/biophysj.104.049866

Indications of membrane potential changes across the membranes of intact bovine chromaffin cells have been recorded using the cell-attached voltage-clamp configuration (Fenwick et al., 1982). In these experiments current waveforms arising from intracellular action potentials could be recorded across the intact patch. More recently, using the cell-attached voltage-clamp configuration, Verheugen and colleagues have used changes in the reversal potential of the voltage-gated K^+ channel to quantitatively estimate whole-cell membrane potential across an intact membrane patch (Verheugen et al., 1995). These data provided early indications that knowledge of the whole-cell membrane potential could be inferred from current recordings made across intact patches. To date the extent to which cell-attached current-clamp measurements reflect the whole-cell membrane potential has not been extensively investigated. In the experiments presented here, we demonstrate the feasibility of noninvasive measurements of both steady-state and dynamic changes in cell membrane potential across an intact membrane patch using the current-clamp mode of a patch-clamp amplifier.

MATERIALS AND METHODS

Reagents

All reagents used in these experiments were purchased from Sigma-Aldrich (Dorset, UK).

Cell culture

Rat basophilic leukemia cells of the RBL-1 clone were obtained from Dr. S. Ikeda (National Institutes of Health, Bethesda, MD) and were propagated in minimal essential medium with added Earles salts (Sigma-Aldrich). The media was supplemented with 10% fetal bovine serum (Sigma-Aldrich), 1% nonessential amino acids (Invitrogen, Paisley, UK), 100 $U \cdot ml^{-1}$ penicillin (Sigma-Aldrich), 50 $\mu g \cdot ml^{-1}$ streptomycin (Sigma-Aldrich), 2 $\mu g \cdot ml^{-1}$ amphotericin (Sigma-Aldrich) and 2 mM L-glutamine (Sigma-Aldrich). Cells were grown at 37°C in a humidified atmosphere of 95% air and 5% CO_2. Suspension cells were used for propagation in all experiments as previously reported (Schofield and Mason, 1996). Cells were normally used 36–48 h after passaging. For experiments, 1-ml aliquots of media containing healthy floating RBL-1 cells were transferred to a 1.5-ml microcentrifuge tube. A small aliquot of this cell suspension was added directly to the experimental chamber for electrophysiological recording when required. All experiments were performed at room temperature.

Megakaryocyte isolation

Adult male Wistar rats were killed by exposure to a rising concentration of CO_2 followed by cervical dislocation. Marrow containing megakaryocytes was isolated from the tibial and femoral bones of the hind limbs into saline containing (in mM) 145 NaCl, 5 KCl, 1 $CaCl_2$, 1 $MgCl_2$, 10 Hepes, 10 D-glucose, pH 7.35 with NaOH, and 0.32–0.64 $U \cdot ml^{-1}$ type VII apyrase (Sigma-Aldrich) as described previously (Mahaut-Smith et al., 1999). Apyrase was present during the isolation and storage of the marrow preparation to degrade spontaneously released adenosine nucleotides, but was absent during experiments. For electrophysiological recordings, a small aliquot of the marrow preparation was added directly to the experimental chamber with megakaryocytes being easily identifiable based upon their large size and polyploidic nucleus. All experiments were performed at room temperature.

Electrophysiological recording

Single electrode recording in RBL-1 cells

Tight-seal whole-cell and cell-attached patch-clamp recordings in voltage- and current-clamp mode were carried out using an Axopatch 200A amplifier (Axon Instruments, Union City, CA). In whole-cell voltage-clamp mode 70–75% series resistance compensation was achieved using the series resistance compensation feature of the 200A amplifier. Two different pipette solutions were used in whole-cell and cell-attached recordings. A KCl-based pipette solution had the following ionic composition (in mM): 150 KCl, 0.15 EGTA, 2 $MgCl_2$, 10 Hepes, pH 7.3 with KOH. A K-glutamate-based pipette solution contained (in mM) 150 K-glutamate, 2 EGTA, 1 $CaCl_2$, 10 Hepes, pH 7.3 with KOH. Experiments were performed in normal external solution of the following composition (in mM): 145 NaCl, 5 KCl, 1 $CaCl_2$, 1 $MgCl_2$, 10 Hepes, 10 D-glucose, pH 7.35 with NaOH. High-K^+ solution was made by replacing 145 mM NaCl with KCl and titrating with KOH ($[K^+] = 154$ mM). Voltage- and current-clamp recordings made with the K-glutamate internal are corrected for an experimentally determined +13 mV junction potential. The experimental chamber was earthed via an Ag/AgCl pellet placed directly in the chamber downstream of the cell.

Amplifier control and data acquisition were performed using Axograph 4.8 software (Axon Instruments) running on a Macintosh computer using a Digidata 1322A 16-bit data acquisition system (Axon Instruments). For identification of whole-cell currents under voltage-clamp, cells were held at −40 mV and 255-ms ramps from −140 to +60 mV were initiated every second. Currents were filtered at 1 kHz using an 8-pole low-pass Bessel filter (Frequency Devices, Haverhill, MA) and acquired to disk at 2 kHz. Single-channel events from cell-attached patches were recorded during 950-ms ramps from +140 to −60 mV pipette potential from a pipette holding potential of +40 mV. Ramps were applied every 3 s. Membrane voltage under current-clamp conditions in both the whole-cell and cell-attached modes was recorded at 2 kHz from either the unfiltered 10-V_m output of the Axopatch 200A amplifier or from the scaled output filtered at 1 kHz. In some experiments the 10-V_m output was filtered at 15 Hz before sampling at 2 kHz. Data were analyzed using Axograph software and IGOR Pro (Wavemetrics, Lake Oswego, OR).

Simultaneous whole-cell voltage-clamp and cell-attached current-clamp recordings in megakaryocytes

Simultaneous whole-cell voltage-clamp and cell-attached current-clamp recordings were performed using two patch-clamp amplifiers. Conventional tight seal whole-cell patch-clamp in voltage-clamp mode was performed using an Axopatch 200A amplifier with a $\beta = 0.1$ headstage configuration, thus enabling whole-cell capacitance compensation of the large megakaryocyte membrane capacitance (Mahaut-Smith et al., 2003). An Axopatch 200A amplifier was used to record from a second electrode in the tight seal cell-attached current-clamp mode. Both electrodes were filled with a KCl-based pipette solution with the following ionic composition (in mM): 150 KCl, 0.1 EGTA, 0.05 K_5-fura-2 salt, 0.05 Na_2GTP, 2 $MgCl_2$, 10 Hepes, pH 7.3 with KOH. Megakaryocyte experiments were carried out in an extracellular solution of the following composition (in mM): 145 NaCl, 5 KCl, 1 $CaCl_2$, 1 $MgCl_2$, 10 Hepes, 10 D-glucose, pH 7.35 with NaOH. Experiments were performed on a microscope equipped for simultaneous recording of single-cell fura-2 fluorescence as previously reported (Mahaut-Smith et al, 1999). Electrophysiological signals were acquired using hardware and software provided by Cairn Research (Faversham, UK). The current record from the whole-cell electrode under voltage-clamp (Axopatch 200B amplifier) was filtered at 30 Hz (Kemo Variable Filter, Beckenham, UK) and recorded by the Cairn software at 60 Hz. The whole-cell membrane

voltage was recorded at 60 Hz from the unfiltered 10-V_m output of the 200A amplifier. Voltage steps were controlled by PClamp 6 (Axon Instruments) running on a second PC. Membrane voltage recorded from the second electrode in the tight seal cell-attached current-clamp configuration was filtered at 30 Hz and recorded at 60 Hz from the scaled output of the Axopatch 200A. All data were further averaged with software to give a 15 Hz acquisition rate for all channels.

Patch electrodes

Fire-polished patch electrodes were constructed from filamented borosilicate glass (Harvard Apparatus, Edenbridge, UK) and had a resistance of ~5–8 MΩ (for use with RBL cells) or 3–6 MΩ (for use with megakaryocytes) when filled with KCl-based internal. For some single-channel recordings electrode shanks were coated with Sylgard 184 silicone elastomer (Dow Corning, Wiesbaden, Germany) to reduce pipette capacitance.

Simultaneous whole-cell voltage-clamp and cell-attached current-clamp recordings in a model circuit

Simulated simultaneous whole-cell voltage-clamp and cell-attached current-clamp recordings in a single cell were made using an equivalent model circuit connected to two patch-clamp amplifiers. The equivalent model circuit used to approximate this experimental situation is presented in Fig. 1 *A* with the actual circuit presented in Fig. 1 *B*. Resistors X_1 and X_2 in this circuit diagram represent the seal resistance and the resistance of the cell-attached patch, respectively, and were altered to experimentally define the relationship between the ratio of these resistances and the fraction of the whole-cell membrane potential recorded across a cell-attached patch. This model circuit deviates from a true equivalent membrane circuit in three ways. First, the circuit does not include a low-value resistor to represent the resistance of the cell-attached electrode. This was neglected as the resistance of this component of the circuit is at least two orders of magnitude less than the patch resistance and thus has negligible impact upon the results. Second, we have designed the circuit to remove series resistance error in voltage-clamping the cell. Third, the whole-cell voltage-clamp component of the equivalent circuit does not contain a high-value resistor in parallel with the cell input resistance representing the seal resistance of the electrode. Since this resistance represents a pathway to earth for current flow it was omitted, indicative of an infinite seal resistance. This minimizes the required holding current passed by the amplifier to clamp the potential of the whole-cell component of the circuit, and its absence has no influence upon the results of the model circuit experiments.

To set the whole-cell potential and simultaneously record this potential across the cell-attached patch, two Axopatch 200A amplifiers (Axon Instruments) were used, with one headstage connected to the cell-attached point in the circuit (Part 2) and the second connected to the whole-cell point in the circuit (Part 1) after the zeroing of the amplifiers using the bath input of the actual circuit (Fig. 1 *B*). The whole-cell amplifier was placed in voltage-clamp, mimicking voltage-clamp control of the cell in the whole-cell configuration, whereas the second amplfier headstage was placed in current-clamp mode, mimicking current-clamp recording across a cell-attached patch in the same cell. Whole-cell membrane potential was altered by manually changing the holding potential while simultaneously recording to disk, using Axograph software, the command potential and the potential from the scaled output of the cell-attached amplifier in current-clamp mode.

Experimental chamber and solution exchange

Cell experiments were performed in a shallow perspex chamber of ~0.5 ml, the bottom of which was formed by adhering a number 1 coverslip with silicone high-vacuum grease. Solution exchange in the experimental chamber was made by gravity fed bath superfusion with solution removal being achieved using a 100 millibar vacuum pump.

RESULTS

Fig. 1 *A* shows a model equivalent circuit for a two-electrode experiment in which one electrode is in voltage-clamp mode in the whole-cell configuration and a second electrode is in current-clamp mode in the cell-attached configuration, as presented in the Methods section. Part 1 of the circuit can be placed under voltage control using a patch-clamp amplifier in voltage-clamp mode positioned at the point of the circuit denoted as whole-cell. Part 2 of the circuit is equivalent to a second patch-clamp electrode in cell-attached mode in the same cell with resistors X_1 and X_2 representing the seal resistance and the patch resistance, respectively. This electrode can be placed in current-clamp mode and the potential across the patch measured. For the purpose of formalizing the theoretical relationship between the seal/patch resistance of the cell-attached component of the circuit and the fraction of the whole-cell command potential measured across the membrane patch ($V_{measure}$), this circuit can be simplified to that presented in Fig. 1 *C*. In this circuit the voltage-clamp command potential is represented by a battery generating a potential difference in the circuit and $V_{measure}$ is the potential recorded by the cell-attached electrode under current-clamp. Assuming that measuring voltage draws no current then the following relationship holds in accordance with Kirchoff's law:

$$\frac{V_{measure}}{X_1} = \frac{V_{command} - V_{measure}}{X_2} \tag{1}$$

Solving for the ratio of V_{meaure} to $V_{command}$ yields the following equation:

$$\frac{V_{measure}}{V_{command}} = \frac{\frac{X_1}{X_2}}{1 + \frac{X_1}{X_2}} \tag{2}$$

This has the form:

$$y = \frac{x}{1 + x} \tag{3}$$

where x is the ratio of the seal/patch resistance and y is the measure of the fraction of the command potential set by whole-cell voltage-clamp (denoted as the battery generating the potential difference in Fig. 1 *C*) measured by the cell-attached current-clamp amplifier. In Fig. 2 *A* the theoretical relationship between the measured potential and the command potential is plotted for seal/patch resistance ratios from zero up to 100. This relationship is defined by a steep increase in the accuracy of the measured potential as the resistance ratio initially increases and the accuracy approaches unity as the resistance ratio approaches infinity.

The accuracy of this predicted relationship was compared with that obtained experimentally using the equivalent circuit shown in Fig. 1 *B*. Two patch-clamp amplifiers were introduced into this circuit; one setting command potentials for the whole-cell configuration and a second measuring potential in current-clamp mode across an intact

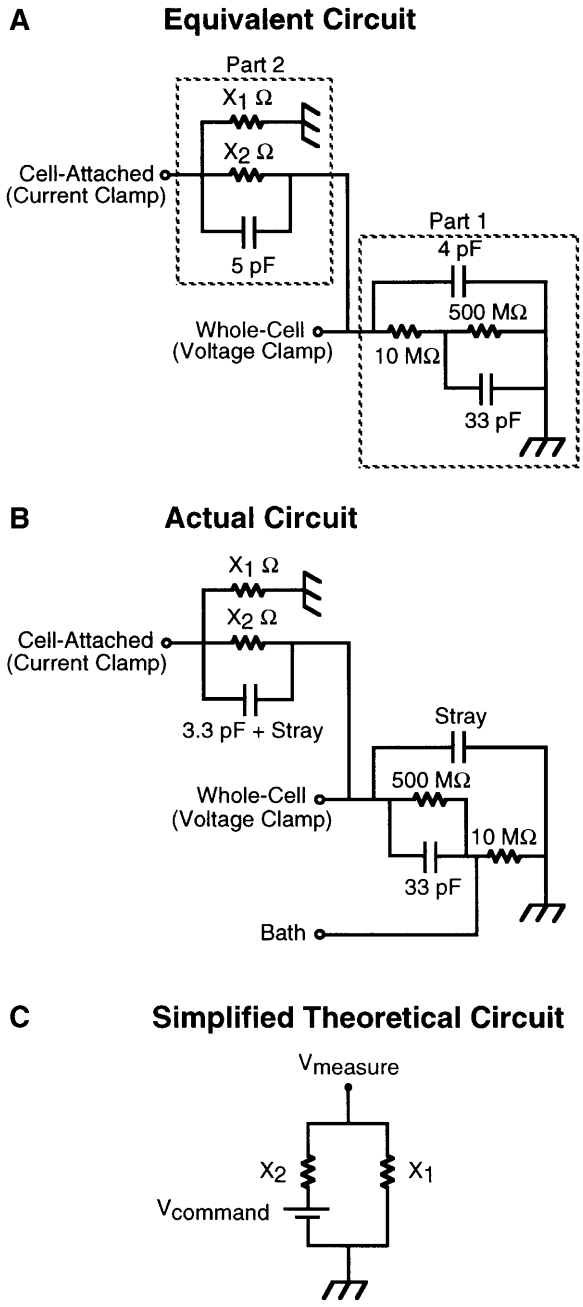

FIGURE 1 Equivalent circuit diagrams denoting simultaneous whole-cell and cell-attached recording from a model cell. (*A*) Equivalent model circuit for simultaneous whole-cell and cell-attached recording from a single cell. Part 1 of the circuit is equivalent to a cell with an input resistance of 500 MΩ and a 33-pF capacitance in series with a 10-MΩ electrode and 4 pF of electrode capacitance in parallel. The circuit is placed in voltage clamp by connecting the headstage of the patch-clamp amplifier to the ''whole-cell'' input. Part 2 of the circuit is equivalent to an infinitely low resistance patch electrode in cell-attached mode in the same cell as denoted by Part 1 of the circuit. Resistors X_1 and X_2 represent the seal and patch resistances, respectively. The circuit can be placed in current-clamp by connecting the headstage of a second patch-clamp amplifier to the ''cell-attached'' input. (*B*) Actual circuit used. The input labeled *Bath* isolates the 10-mΩ whole-cell electrode from the rest of the circuit for the purpose of nulling the current flow across the electrodes before placing the circuit under clamp. (*C*) Simplified theoretical circuit representing the recording of potential across a membrane patch (X_2) using the tight-seal patch-clamp configuration in current-clamp mode. X_1 is the seal resistance through which current can flow to earth.

membrane patch on the same cell. Fig. 2 *B* shows the relationship between $V_{command}$ (the whole-cell membrane potential set by voltage-clamp) and $V_{measure}$ (the potential recorded across the cell-attached patch) for nine different ratios of seal/patch resistance. The slope of the linear fit to each data set, $V_{measure}/V_{command}$, is equivalent to the fractional accuracy of the cell-attached recording under the defined conditions of seal and patch resistance. In Fig. 2 *C*, the relationship between the fractional accuracy of the current-clamp measurement as a function of the nine seal/patch resistance ratios is superimposed upon the theoretical relationship presented in Fig. 2 *A*. The experimentally derived relationship agrees extremely well with the theoretically predicted response. From these data one can see that a seal to patch resistance ratio of 3 is sufficient to allow recording of 75% of the cell membrane potential across the intact membrane patch.

To investigate the usefulness of this technique, measurements of membrane potential were performed in RBL-1 cells. As a result of the small size of the RBL-1 cell it was not possible to reliably perform simultaneous whole-cell and cell-attached experiments. Rather, potential was recorded under current-clamp in cell-attached mode immediately before obtaining the whole-cell configuration and recording membrane potential again under current-clamp. Paired values for steady-state membrane potential recorded in the cell-attached and whole-cell configuration were obtained in 24 cells. Fourteen cells were depolarized (i.e., less negative) in both the cell-attached and whole-cell configuration whereas 10 cells showed a hyperpolarized potential when recorded in the cell-attached configuration. Of these 10 cells, eight were still hyperpolarized when potential was recorded in the whole-cell configuration. The two remaining cells were depolarized, possibly a result of alterations in the whole-cell currents or seal resistance during the transition to the whole-cell mode. Data from these two cells are excluded from the membrane potential values summarized in Table 1. These data demonstrate that in hyperpolarized cells 77% of the membrane potential recorded in the whole-cell mode is recorded across the cell-attached patch. In addition, no significant difference in the potential recorded by the two configurations was detected in depolarized cells.

To investigate the ability of cell-attached current-clamp recordings to measure dynamic changes in membrane potential, cells were reversibly depolarized by superfusion with a saline solution containing 154 mM K^+. A representative experiment is shown in Fig. 3. Application of high-K^+ saline to hyperpolarized cells resulted in a depolarization to $\sim+2$ mV when recorded under current clamp in the cell-attached configuration. This depolarization was fully reversible upon removal of the high-K^+ saline. After the transition to the

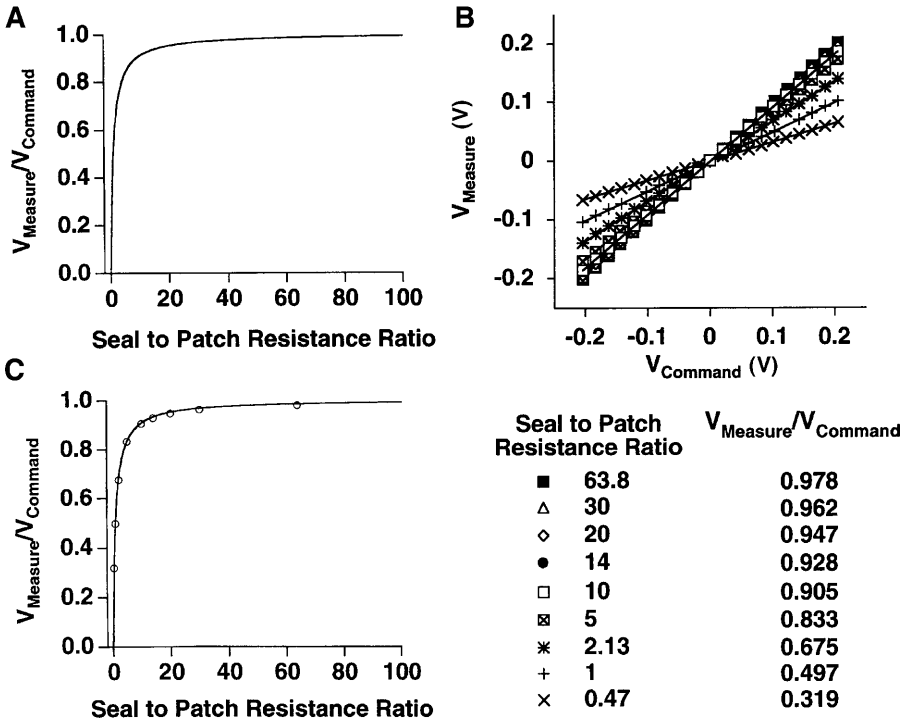

FIGURE 2 The theoretical and experimental relationships between cell-attached current-clamp measurements of membrane potential ($V_{measure}$) and whole-cell voltage-clamp command potential as a function of the seal/membrane patch resistance ratio of the cell-attached configuration. (*A*) The theoretical relationship between $V_{measure}$ and $V_{command}$ as a function of seal/patch resistance ratios from 0 to 100 for the cell-attached configuration denoted by Fig. 1 *C*. (*B*) Experimental determination of the relationship between $V_{measure}$ and $V_{command}$ as a function of nine seal/patch resistance ratios. The ratios were obtained by varying the resistances of X_1 and X_2 in the circuit shown in Fig. 1 *B*. Each series of data were fit to a line with the slope of the line, $V_{measure}/V_{command}$, and the corresponding resistance ratio denoted in the table. (*C*) The experimentally derived data from panel *B* is superimposed upon the theoretical relationship derived in panel *A*.

whole-cell configuration, the resting potential was ~10 mV more hyperpolarized with the response to high-K^+ exposure being virtually identical. It was consistently found that the high-frequency noise evident upon the cell-attached records was dramatically reduced upon transition to the whole-cell configuration. This observation was very useful in monitoring the integrity of the cell-attached configuration. Table 2 summarizes the membrane potential readings from unpaired cell-attached and whole-cell recording made immediately before and at the peak of exposure to high-K^+ saline.

Although the presence of high-frequency noise on the membrane potential trace was a useful indication of the configuration of the recording, it was necessary to ensure that the cell-attached measurements were in fact measured across an intact patch and not across a partially perforated patch. Under these ionic conditions, the detection of single-channel events in the RBL-1 cell can only be observed in an intact cell-attached configuration. Therefore, detection of channel events is a definitive indication of the patch integrity. To confirm the integrity of the cell-attached configuration, single-channel recordings were made before switching to

TABLE 1 Paired current-clamp measurements of the potential recorded across a cell-attached patch and in the whole-cell configuration in RBL-1 cells

	Cell-attached	Whole-cell
Hyperpolarized ($n = 8$)	−57.4 ± 4.5	−74.5 ± 4.9*
Depolarized ($n = 14$)	−10.2 ± 2.6	−9.4 ± 1.9

Current-clamp measurements of membrane potential were recorded in the cell-attached configuration immediately before the transition to the whole-cell configuration and the current-clamp measurement of potential in the whole-cell mode. The pipette internal had the following composition (in mM): 150 K-glutamate, 2 EGTA, 1 $CaCl_2$, 10 Hepes, pH 7.3 with KOH. Potentials have been corrected for a +13 mV liquid junction potential.
*Statistically different from the potential recorded in the cell-attached configuration ($P \leq 0.01$).

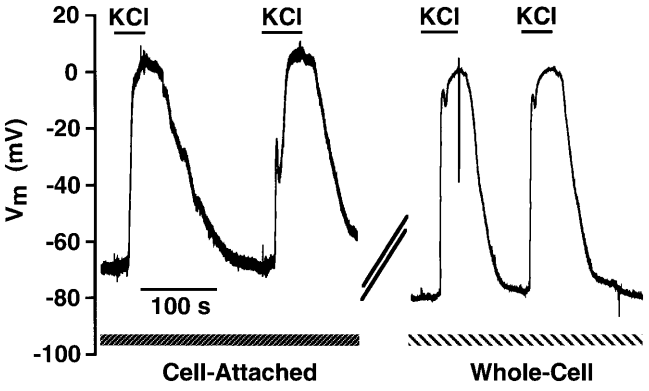

FIGURE 3 Measurement of RBL-1 membrane potential in the cell-attached and whole-cell configurations. The cell was superfused with an external solution containing (in mM) 145 NaCl, 5 KCl, 1 $CaCl_2$, 1 $MgCl_2$, 10 Hepes, 10 D-glucose, pH 7.35 with NaOH. Membrane potential was first recorded across a cell-attached patch using the patch-clamp amplifier in the current-clamp mode and a pipette solution of the following composition (in mM): 150 K-glutamate, 2 EGTA, 1 $CaCl_2$, 10 Hepes, pH 7.3 with KOH. During the break in the trace (266 s), the electrode was placed into voltage clamp and a transition to the whole-cell configuration was made. The amplifier was then placed back into current-clamp and the potential recorded. Where indicated, an extracellular solution containing 154 mM K^+ was superfused into the experimental chamber. Data are corrected for a +13 mV liquid junction potential.

TABLE 2 Unpaired current-clamp measurements of the potential recorded across a cell-attached patch and in the whole-cell configuration during application of high-K^+ solution

KCl	Cell-attached ($n = 13$)	Whole-cell ($n = 10$)
−	−62.8 ± 2.4	−81.3 ± 1.8*
+	3.2 ± 1.2	−3.0 ± 1.7*

Current-clamp measurements of membrane potential were recorded in the cell-attached configuration during application of high-K^+ solution (154 mM) and the mean potential immediately before and at the peak of high-K^+-induced depolarization was measured. The cell was then placed in the whole-cell configuration and current-clamp recordings of membrane potential in response to high-K^+ application were again measured. The pipette internal had the following composition (in mM): 150 K-glutamate, 2 EGTA, 1 $CaCl_2$, 10 Hepes, pH 7.3 with KOH. Potentials have been corrected for a +13 mV liquid junction potential.
*Statistically different from the potential recorded in the cell-attached configuration ($P \leq 0.01$).

current-clamp mode to record membrane potential. The pipette potential was held at +40 mV under voltage-clamp and ramps of 900-ms duration from +140 mV to −60 mV pipette potential were initiated every 3 s. Four representative ramps are shown in Fig. 4 *A*. For clarity, the capacitative transient accompanying the step from +40 to +140 in the non-Sylgarded electrode has been truncated. Clear single-channel opening and closing events are evident in episodes 22, 24, and 27, consistent with the integrity of the cell-attached patch. The electrode was placed in current-clamp mode and the potential across the cell-attached patch was recorded in response to application of high K^+-containing saline (Fig. 4 *B*). In additional experiments single-channel events were recorded after cell-attached current-clamp recording of the response to high-K^+ saline, with identical results (data not shown). Taken in concert, these data confirm that the cell-attached recordings of potential are being made across an intact membrane patch.

During cell-attached current-clamp recordings in partially depolarized cells, application of high K^+ showed complex changes in potential. During K^+ application a transient hyperpolarization was frequently observed before a depolarization to a value expected from application of 154 mM K^+ (Fig. 5 *A*; see *inset* for expanded section of trace showing transient hyperpolarization). This was first considered a possible artifact associated with the cell-attached recording of potential. However, this is not the case as identical transient hyperpolarizations could be seen in partially depolarized cells during whole-cell current-clamp recordings, as shown in Fig. 5 *B*. Further anomalous behavior is observed upon returning the cell to normal saline. Removal of high K^+ resulted in a large hyperpolarization of the cell to a value approximating that detected in hyperpolarized cells (Tables 1 and 2). This was followed by a rapid transitional change in potential back to the depolarized state.

It is important to realize that superfusion of high-K^+ saline into the experimental chamber does not result in an instantaneous change in extracellular K^+. Mixing occurs in the chamber and the [K^+] in the vicinity of the cell rises to the new value of 154 mM with a time constant dependent upon the rate of solution flow, conditions of mixing in the chamber, and the position of the cell in the chamber. This is evident from the time course of the change in potential recorded in the whole-cell mode in Fig. 3. An investigation of the whole-cell current changes during application of high K^+ was undertaken in an effort to explain these anomalous changes in potential. Current-clamp measurements were first made in the whole-cell configuration in depolarized cells to confirm the presence of the anomalous changes in potential

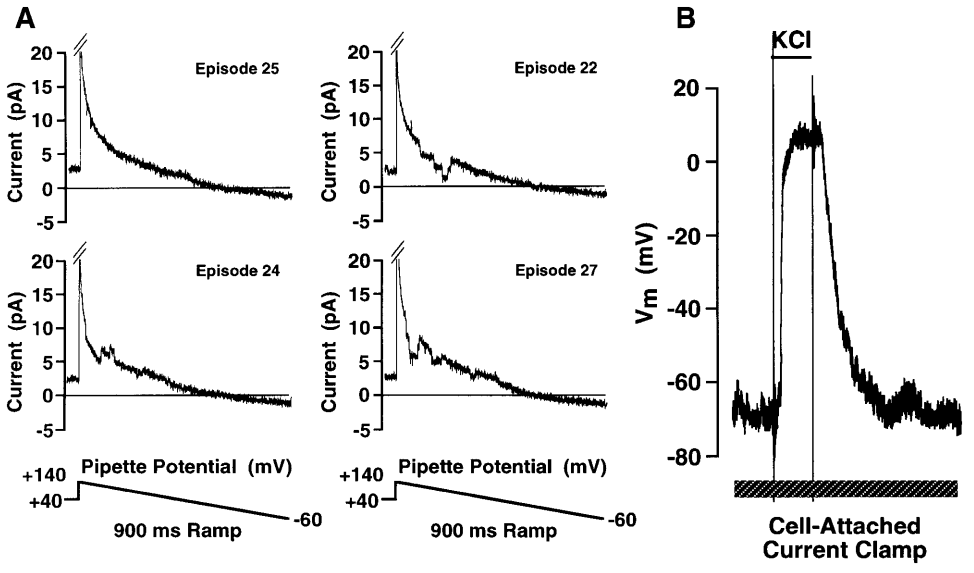

FIGURE 4 The detection of single-channel events in RBL-1 cells before the measurement of membrane potential across the cell-attached patch. (*A*) Single-channel events from cell-attached patches were recorded during 950-ms ramps from +140 to −60 mV applied pipette potential from a pipette holding potential of +40 mV. Ramps were applied every 3 s. The cell was superfused with an external solution containing (in mM) 145 NaCl, 5 KCl, 1 $CaCl_2$, 1 $MgCl_2$, 10 Hepes, 10 D-glucose, pH 7.35 with NaOH. The pipette solution had the following composition (in mM): 150 KCl, 0.15 EGTA, 2 $MgCl_2$, 10 Hepes, pH 7.3 with KOH. (*B*) After collection of single-channel data the amplifier was placed in current-clamp mode and membrane potential was recorded. Where indicated, an extracellular solution containing 154 mM K^+ was superfused into the experimental chamber.

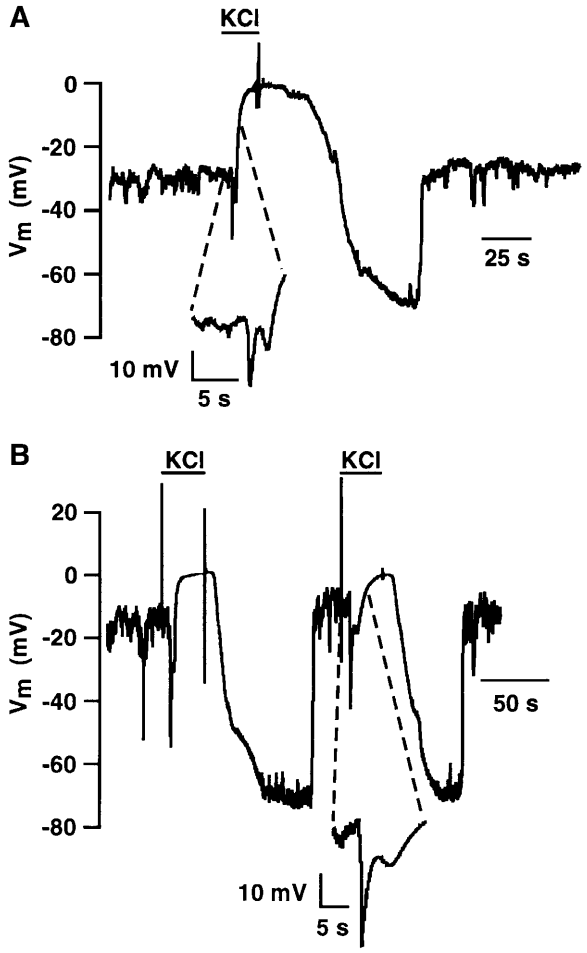

FIGURE 5 Cell-attached and whole-cell recording of membrane potential in partially depolarized RBL-1 cells during exposure to high K^+. (*A*) An RBL-1 cell was superfused with normal external saline (in mM): 145 NaCl, 5 KCl, 1 $CaCl_2$, 1 $MgCl_2$, 10 Hepes, 10 D-glucose, pH 7.35 with NaOH, and membrane potential was recorded across a cell-attached patch using a K-glutamate-based internal (in mM): 150 K-glutamate, 2 EGTA, 1 $CaCl_2$, 10 Hepes, pH 7.3 with KOH. Where indicated, a high K^+-based external saline (154 mM K^+) was superfused into the chamber. The inset shows the initial response to application of high K^+ at higher temporal resolution. Data are corrected for a +13 mV liquid junction potential. (*B*) A different RBL-1 cell was superfused with normal external saline (in mM): 145 NaCl, 5 KCl, 1 $CaCl_2$, 1 $MgCl_2$, 10 Hepes, 10 D-glucose, pH 7.35 with NaOH, and membrane potential was recorded under current-clamp in the whole-cell configuration using a KCl-based pipette internal (in mM): 150 KCl, 0.15 EGTA, 2 $MgCl_2$, 10 Hepes, pH 7.3 with KOH. Where indicated a high K^+-based external saline (154 mM K^+) was superfused into the chamber. The inset shows the initial response to application of high K^+ at higher temporal resolution.

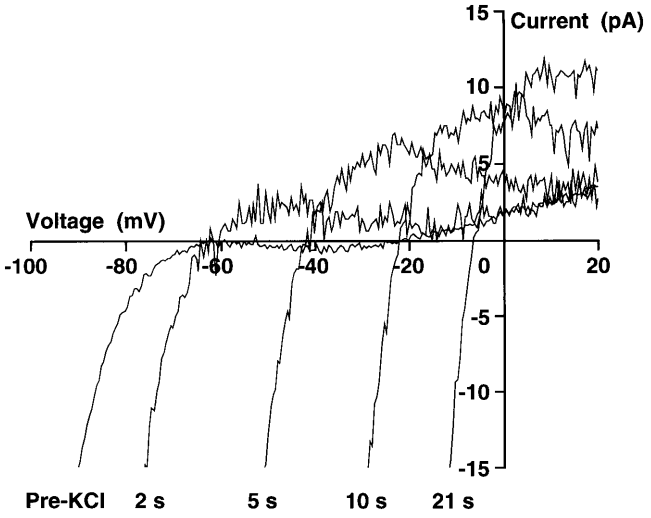

FIGURE 6 Whole-cell ramp currents recorded in an RBL-1 cell during application of high-K^+ solution. The whole-cell voltage-clamp configuration was obtained using a KCl-based pipette solution (in mM): 150 KCl, 2 EGTA, 1 $CaCl_2$, 10 Hepes, pH 7.3 with KOH. Ramps of 200-ms duration from −140 to +60 mV were applied at 1-s intervals from a holding potential of −40 mV while the cell was superfused with normal saline (in mM): 145 NaCl, 5 KCl, 1 $CaCl_2$, 1 $MgCl_2$, 10 Hepes, 10 D-glucose, pH 7.35 with NaOH. The current record, labeled *Pre-KCl*, is the average of 16 ramps taken immediately before the first change in null current potential recorded during superfusion with 154 mM KCl solution. Whole-cell currents are shown 2, 5, 10, and 21 s after superfusion of high-K^+ solution.

in response to addition and removal of high extracellular [K^+]. The cell was then placed in voltage clamp and held at −40 mV. Ramps of 255-ms duration from −140 to +60 mV were initiated every second. The *I-V* curve labeled *Pre-KCl* in Fig. 6 is the average whole-cell recording from 16 ramps taken immediately before application of high-KCl saline and displays the characteristics of the dominant inwardly rectifying K^+ current present in RBL cells (Lindau and Fernandez, 1986; McCloskey and Cahalan, 1990; Mukai et al., 1992, Mason et al., 1999). A close inspection of the null current value indicates that the membrane potential would be ~−21 mV, consistent with the depolarized nature of the cell when recorded under current clamp. This arises as a result of the lack of an outward current component to the *I-V* relationship at more negative potentials. The current-voltage relationships labeled 2 s, 5 s, 10 s, and 21 s were obtained at those times after the first detected change in the *I-V* relationship in response to changing to a solution containing 154 mM K^+. During superfusion of high K^+, there is an increase in the slope conductance of the inwardly rectifying K^+ channel *I-V* curve at negative potentials and, importantly, an increase in the outward component of the *I-V* relationship, observations previously reported in response to increasing extracellular [K^+] (Lindau and Fernandez, 1986; McCloskey and Qian, 1994; Kelly et al., 1992). The effect of the increase in outward component of the *I-V* relationship is to transiently shift the null current potential toward a hyperpolarized potential set by the K^+ equilibrium potential. As discussed above, the extracellular [K^+] does not change instantaneously, but rather, increases slowly as a result of mixing. A modest increase in extracellular [K^+] is sufficient to increase the outward component of the *I-V* relationship but still results in a hyperpolarized K^+ equilibrium potential. As the extracellular [K^+] continues to rise, the null current potential depolarizes in accordance with the changing K^+

equilibrium potential. Under current-clamp conditions this is expected to result in a rapid transient hyperpolarization followed by depolarization toward a potential set by the final extracellular [K^+] of 154 mM, consistent with the membrane potential changes presented in Fig. 5. This would be expected to occur in reverse upon returning to normal saline. Therefore, the noninstantaneous exchange of solution in the chamber and the resultant transient changes in the outward current component of the inwardly rectifying K^+ channel most likely underlie the anomalous changes in membrane potential recorded in Fig. 5. Importantly, these changes are faithfully recorded across the cell-attached patch, as is evident in Fig. 5 *A*.

As is clear from the data presented in Fig. 2, the accuracy of the membrane potential measured across an intact membrane patch is dependent upon obtaining a low-resistance patch and a high seal resistance. The rat megakaryocyte has a complex membrane architecture referred to as the demarcation membrane (Behnke 1968; Yamada, 1957). This membrane is electrically coupled to the plasma membrane, suggesting that a conventional cell-attached patch might possibly be electrically coupled to far more membrane than predicted from the area of the patch (Mahaut-Smith et al., 2003). Theoretically, this increase in membrane would be expected to reduce the resistance of the patch, thereby making it an excellent candidate for further investigations into the feasibility of potential recordings across a cell-attached patch. In addition, the large size of the megakaryocyte facilitates two electrode patch-clamp experiments so that the two-electrode configuration denoted by the model circuit of Fig. 1 can be achieved in a biological sample. Experiments were undertaken to investigate the accuracy of cell-attached membrane potential measurements in these large cells. Simultaneous cell-attached and whole-cell recordings were obtained in four cells. In three of these cells a high-resistance seal was obtained with both electrodes whereas low-resistance seals were obtained in one cell. Fig. 7 shows a representative experiment with two high-resistance seals. Whole-cell potential was either measured under current-clamp or controlled by voltage-clamp while membrane potential was simultaneously recorded across an intact patch using a second electrode in current-clamp mode. The cell was initially held at −75 mV with ~70% series resistance compensation and the cell-attached potential recorded was ~2 mV more negative (−77 mV). A change in holding potential to 0 mV was accompanied by a rapid initial depolarization of the cell-attached recording followed by a secondary slower further increase to a value approaching 0 mV. This secondary slower change in potential mirrored the inactivation of the large outward voltage-gated K^+ current and most likely represents the true whole-cell voltage as a result of uncompensated series resistance. The whole-cell electrode was placed in current-clamp mode and a spontaneous transient hyperpolarization was detected on both electrodes, consistent with a transient rise in [Ca^{2+}]$_i$ and

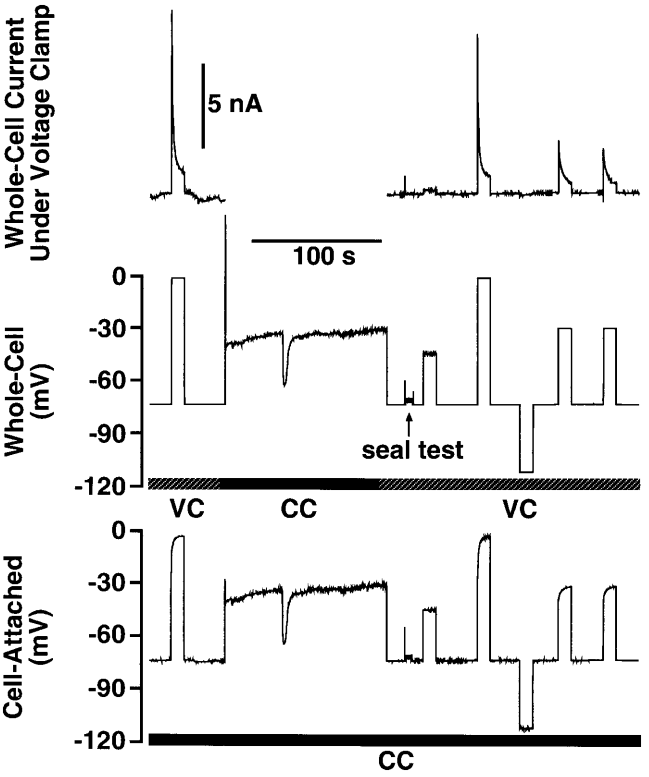

FIGURE 7 Simultaneous cell-attached current-clamp and whole-cell voltage-clamp recordings in a rat megakaryocyte. (*Upper panel*) Membrane currents recorded under whole-cell voltage-clamp during superfusion with normal saline solution: 145 NaCl, 5 KCl, 1 $CaCl_2$, 1 $MgCl_2$, 10 Hepes, 10 D-glucose, pH 7.35 with NaOH. The pipette contained (in mM) 150 KCl, 0.1 EGTA, 0.05 fura-2 penta K^+ salt, 0.05 Na_2GTP, 2 $MgCl_2$, 10 Hepes, pH 7.3 with KOH. (*Middle panel*) Holding potential set by whole-cell voltage-clamp (*VC*). Where indicated the cell was placed in current-clamp (*CC*) and membrane potential was recorded. Where noted, a seal test was performed and the capacitative transients were adjusted. (*Bottom panel*) Simultaneous current-clamp recording (*CC*) of membrane potential measured across an intact cell-attached patch in the same cell. The pipette contained the same internal as used for the whole-cell recordings.

the activation of Ca^{2+}-gated K^+ channels (Uneyama et al., 1993a,b; Mason et al., 2000). The cell was returned to whole-cell voltage-clamp and a holding potential of −75 mV. Voltage steps, both depolarizing and hyperpolarizing, were made while recording the potential across the cell-attached patch. Changes in holding potential that did not activate large membrane currents were faithfully mirrored by the cell-attached electrode. Only when large membrane currents were activated by the voltage steps was a biphasic change in potential recorded by the cell-attached electrode. These data further support the conclusion that the biphasic potential change is a true indication of the whole-cell potential arising from the uncompensated component of the series resistance. It is important to note that under conditions where no large membrane currents are activated, the voltage excursions recorded across the cell-attached patch were virtually identical to the voltage step applied under voltage clamp. This high degree of accuracy of measurement of

membrane potential by the cell-attached electrode was observed in all three cells in which high-resistance seals were obtained and is consistent with a large seal/patch resistance ratio. In the cell in which low-resistance seals were obtained, whole-cell current-clamp recordings revealed spontaneous oscillations in potential driven by oscillations in $[Ca^{2+}]_i$ and the activation and inactivation of Ca^{2+}-activated K^+ channels, as discussed above. Despite the low-resistance seal, the oscillations, including the inherent variability in their magnitude, were faithfully recorded by the cell-attached electrode. As expected, both the absolute magnitude of the oscillations and the resting potential recorded with the cell-attached electrode were significantly less than that recorded by the whole-cell electrode, as predicted by the much lower seal/patch resistance ratio.

We have previously reported adenosine diphosphate (ADP) mediated oscillations in $[Ca^{2+}]_i$ and membrane potential under whole-cell current-clamp conditions in rat megakaryocytes (Somasundaram and Mahaut-Smith, 1995; Mason et al.,2000). A major concern of these experiments is that dialysis of the cell with the pipette solution is contributing to the oscillatory nature of the response. To address this question, experiments were undertaken to monitor membrane potential using a cell-attached electrode during application of ADP. In eight out of nine cells oscillations in membrane potential were recorded in response to ADP exposure. A representative experiment is shown in Fig. 8. Superfusion with 1 μM ADP resulted in oscillations in membrane potential between a resting potential of ~ -40 mV and a value of ~ -70 mV. Resting potential, the magnitude of the oscillations, and the kinetics of the oscillations were indistinguishable from oscillations recorded in the whole-cell configuration (Mahaut-Smith et al., 1999; Mason et al.,2000). Thus, cell dialysis does not underlie the oscillatory nature of the response. These experiments highlight the usefulness of cell-attached current-clamp recordings for noninvasive detection of dynamic changes in membrane potential.

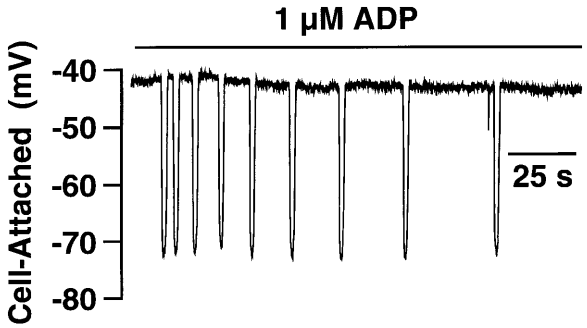

FIGURE 8 Cell-attached current-clamp measurements of membrane potential in response to ADP application. Where indicated, the cell was superfused with 1 μM ADP in saline containing (in mM) 145 NaCl, 5 KCl, 1 $CaCl_2$, 1 $MgCl_2$, 10 Hepes, 10 D-glucose, pH 7.35 with NaOH. The pipette contained (in mM) 150 KCl, 0.1 EGTA, 0.05 fura-2 penta K^+ salt, 0.05 Na_2GTP, 2 $MgCl_2$, 10 Hepes, pH 7.3 with KOH.

DISCUSSION

In these experiments, we have exploited the use of the current-clamp mode of a conventional patch-clamp amplifier to monitor membrane potential across an intact membrane patch. The theoretical solution to the equivalent model circuit presented in Fig. 1 indicated that the relationship between the seal/patch resistance ratio and the accuracy of recorded potential across a cell-attached patch increases rapidly as the seal/patch resistance ratio of the cell-attached component of the equivalent circuit increases. The accuracy of this relationship was confirmed experimentally by introducing two patch-clamp amplifiers into the circuit; one for the purpose of gaining voltage control and the second for the purpose of recording potential across the equivalent membrane patch. Using RBL-1 cells, the feasibility of cell-attached recordings of membrane potential were confirmed. Surprisingly, 77% of the whole-cell membrane potential was recorded across an intact membrane patch (Tables 1 and 2), indicative of a seal/patch ratio of 3.3 as determined by the solution to the equivalent circuit model presented in Fig. 2. Using this value one can, in principle, correct potential recorded across a cell-attached patch to give an estimate of the true whole-cell potential. Far more importantly, measurements across an intact patch, irrespective of the degree of absolute accuracy, mirror dynamic changes in potential recorded whole-cell, thus enabling this type of recording to be used to investigate the dynamics of membrane potential in a noninvasive manner. This is particularly useful, as dialysis of the cytosol which occurs under whole-cell conditions and ionic changes accompanying perforated patch recordings may have a profound influence upon membrane potential.

When recording dynamic changes in potential using this technique it is important to consider the speed of the changes. Two issues arise. First, the design of many patch-clamp amplifiers, that enables them to monitor potential using the current-clamp mode, has limitations in the recording of high-frequency changes in potential (Magistretti et al, 1996,1998). This is a major problem for quantitative analysis of membrane potential in excitable cells where action potentials and burst-firing have high-frequency components to their signal. This is a general problem associated with current-clamp measurements using conventional patch-clamp amplifiers and is not confined to the cell-attached configuration. However, in nonexcitable cells there is a greatly reduced high-frequency component in the membrane potential signal making current-clamp measurements less prone to the artifacts present in measurements in excitable cells. Second, the capacitance elements of the cell-attached recording of potential effectively act as low-pass filters that attenuate high-frequency signal components. With the availability of patch-clamp amplifiers with true

current-clamp circuits the concerns raised by point 1 are muted. However, concerns raised by the filtering influences of the capacitance elements of the cell-attached recording remain. We have calculated the step response of the equivalent circuit presented in Fig. 1 *A*. The time constant of the change in potential recorded by the cell-attached electrode in response to a step change in whole-cell potential is given by the following relationship:

$$\tau = \frac{R_m \times C_m \times (R_m + R_{seal})}{R_{seal}} \quad (4)$$

where R_m, C_m, and R_{seal} are the patch resistance, the patch capacitance, and the seal resistance, respectively. It is clear from this relationship that when the seal/patch resistance ratio approaches infinity, the time constant is simply the product of the patch resistance and capacitance. Thus, an upper limit of the frequency response of the cell-attached configuration can be estimated from these parameters. Even under ideal conditions of an infinite seal/patch resistance ratio the constraints of the patch resistance and its associated capacitance mean that very rapid changes in potential such as action potentials cannot be faithfully recorded. However, the relatively low bandwidth changes associated with nonexcitable cells will be faithfully recorded. With our estimated seal/patch resistance relationship of 3.3 the time constant is only increased by a further 30%, ensuring faithful recording of signals below a −3-dB corner frequency of ~120 Hz if the product of the patch resistance and capacitance was 1 ms.

It is important to bear in mind that even small headstage offset currents can result in dramatic errors in cell-attached measurements of potential as a result of the high resistance of the membrane patch. Headstage offset currents and leakage currents in current-clamp mode must be offset frequently to ensure that large errors are not introduced.

The high-resistance seals, which are required for good patch-clamp recordings, contributed to the relatively high seal/patch ratio of 3.3 estimated in the RBL-1 cell. Interestingly, all of our measurements of single-channel events in RBL-1 cells revealed multiple channels per patch with a high open probability as determined by the lack of complete closed channel events. Therefore, it seems likely that a low patch resistance in the RBL-1 cells is a contributing factor for the relatively efficient detection of the whole-cell potential. Interestingly, previous estimates in adrenal chromaffin cells by Fenwick and colleagues (1982) indicate that the membrane resistance is much lower than predicted from the ratio of patch area to membrane surface area. The authors propose that the process of forming a high-resistance seal may in fact be responsible for lowering the patch resistance, possibly via membrane damage. However, should membrane damage underlie the low resistance achieved in RBL cells it does so without compromising the ability to detect single-channel events, thus ensuring that the cell-attached configuration is intact.

Opening and closing events in patches containing a low channel density will undergo large changes in patch resistance that will show up as rapid transitional changes in potential as the fractional accuracy of the recorded membrane potential is altered with changing resistance. The rapid fluctuations in potential recorded in partially depolarized cells in the cell-attached configuration (Fig. 5 *A*) were first thought to be as a result of such events. However, this does not appear to be the case as similar transitions were recorded in the whole-cell configuration (Fig. 5 *B*). These fluctuations in potential most likely arise from the inherent instability of the null current potential of depolarized cells. This instability arises as a result of 1), the small peak outward current between −80 and −40 mV; and 2), the decline in the outward current between −60 and −40 mV. As a result, small alterations in membrane current can result in pronounced shifts in potential to a new null current potential (Mason et al., 1999). The origin of the current changes responsible for the instability of the membrane potential observed in Fig. 5 may lie at the level of endogenous membrane currents or at the level of alterations in the seal resistance of the whole-cell or cell-attached electrode.

In the case of the megakaryocytes, membrane potential recorded across patches approached that set by whole-cell voltage-clamp. The presence of the demarcation membrane which is electrically coupled to the plasma membrane (Mahaut-Smith et al., 2003) may help explain this high degree of accuracy of the detection of potential. This increase in membrane may be significantly reducing the effective patch resistance and therefore increasing the seal/patch resistance ratio to a much higher value than that obtained in the absence of demarcation membrane. However, further experiments are required to define the role of this platelet precursor membrane system in the high degree of accuracy recorded by the cell-attached electrode. As a potential use of this technique we have exploited cell-attached current-clamp measurements to ensure that the dynamic changes in membrane potential induced by ADP are in fact not an artifact of whole-cell recordings. Although the high degree of accuracy of the membrane potential recorded may be a result of the presence of the demarcation membrane system, the accuracy of the dynamic changes is independent of the presence of a low-resistance patch. Even measurements with low-resistance cell-attached seals faithfully mirrored the dynamic changes recorded whole-cell (data not shown). Therefore, the ability to faithfully measure complex changes in potential is not confined to cells in which a very low-resistance patch is achieved. Thus, this technique will be useful for monitoring dynamic changes in potential under conditions where the accuracy of the absolute values of potential are less important.

As noted above, accurate measurement of membrane potential across a cell-attached patch requires a patch displaying a constant low resistance. Nystatin and amphotericin have been used to reduce patch resistance for the purpose of

obtaining adequate voltage control of the cell under voltage clamp (Horn and Marty, 1988; Rae et al., 1991). Nystatin and amphotericin can also be used to improve the accuracy of the recorded potential in current-clamp mode. However, although these agents will reduce the resistance of the patch, they do so by introducing exogenous channels with high permeability, thus requiring careful consideration of the ionic composition of the patch pipette and the impact of this ionic composition on cell potential after reaching steady-state conditions across the patch. We have performed our experiments without exogenously altering the patch resistance with a surprisingly high degree of accuracy.

These experiments highlight the feasibility of using a cell-attached electrode in current-clamp to measure a large fraction of the whole-cell transmembrane potential non-invasively under steady-state and dynamic conditions. The usefulness and future application of this method will be very much dependent upon the membrane characteristics of the cell under investigation. Numerous factors need to be considered when applying this technique, including 1), the seal/patch resistance ratio under your experimental conditions; 2), the stability of the patch and seal resistances; and 3), the kinetics of the changes in potential. All of these factors will determine the accuracy of the recorded potential. In the RBL cell and the rat megakaryocyte this technique has already proved highly useful for investigations of dynamic changes in potential under noninvasive conditions.

We thank Mick Swann and Simon Reitter for their help and advice with the building of the model circuit and Jon Holdich for expert technical assistance.

This work was funded in part by grants from the Medical Research Council (G9901465 to M.P.M.-S. and M.J.M), the British Heart Foundation (BS10 to M.P.M.-S.), and the Royal Society (M.P.M.-S.).

REFERENCES

Behnke, O. 1968. An electron microscope study of the megakaryocyte of the rat bone marrow. I. The development of the demarcation membrane system and the platelet surface coat. *J. Ultrastruct. Res.* 24:412–433.

Catterall, W. A., R. Ray, and C. S. Morrow. 1976. Membrane potential dependent binding of scorpion toxin to action potential Na^+ ionophore. *Proc. Natl. Acad. Sci. USA.* 73:2682–2686.

Ehrenberg, B., V. Montana, M. Wei, J. P. Wuskell, and L. M. Loew. 1988. Membrane potential can be determined in individual cells from the Nernstian distribution of cationic dyes. *Biophys. J.* 53:785–794.

Fenwick, E. M., A. Marty, and E. Neher. 1982. A patch-clamp study of bovine chromaffin cells and of their sensitivity to acetylcholine. *J. Physiol.* 331:577–597.

Grinstein, S., J. D. Goetz, and A. Rothstein. 1984. $^{22}Na^+$ fluxes in thymic lymphocytes. I. Na^+/Na^+ and Na^+/H^+ exchange through an amiloride-insensitive pathway. *J. Gen. Physiol.* 84:565–584.

Hamill, O. P., A. Marty, E. Neher, B. Sakmann, and F. J. Sigworth. 1981. Improved patch clamp techniques for high resolution current recording from cells and cell-free membrane patches. *Pflugers Arch.* 391:85–100.

Horn, R., and A. Marty. 1988. Muscarinic activation of ionic currents measured by a new whole-cell recording method. *J. Gen. Physiol.* 92: 145–159.

Kao, W. Y., C. E. Davis, Y. I. Kim, and J. M. Beach. 2001. Fluorescence emission spectral shift measurements of membrane potential in single cells. *Biophys. J.* 81:1163–1170.

Kelly, M. E. M., S. J. Dixon, and S. M. Sims. 1992. Inwardly rectifying potassium current in rabbit osteoclasts: A whole-cell and single-channel study. *J. Membr. Biol.* 126:171–181.

Lichtshtein, D., H. R. Kaback, and A. J. Blume. 1979. Use of a lipophilic cation for the determination of membrane potential in neuroblastoma-glioma hybrid cell suspensions. *Proc. Natl. Acad. Sci. USA.* 76:650–654.

Lindau, M., and J. M. Fernandez. 1986. A patch-clamp study of histamine-secreting cells. *J. Gen. Physiol.* 88:349–368.

London, J. A., L. B. Cohen, and Y. J. Wu. 1989. Optical recordings of the cortical response to whisker stimulation before and after addition of an epileptogenic agent. *J. Neurosci.* 9:2182–2190.

Magistretti, J., M. Mantegazza, M. de Curtis, and E. Wanke. 1998. Modalities of distortion of physiological voltage signals by patch-clamp amplifiers: A modeling study. *Biophys. J.* 74:831–842.

Magistretti, J., M. Mantegazza, E. Guatteo, and E. Wanke. 1996. Action potentials recorded with patch-clamp amplifiers: are they genuine? *Trends Neurosci.* 19:530–534.

Mahaut-Smith, M. P., J. F. Hussain, and M. J. Mason. 1999. Depolarization-evoked Ca^{2+} release in a non-excitable cell, the rat megakaryocyte. *J. Physiol.* 515:385–390.

Mahaut-Smith, M. P., D. Thomas, A. B. Higham, J. A. Usher-Smith, J. F. Hussain, J. Martinez-Pinna, J. N. Skepper, and M. J. Mason. 2003. Properties of the demarcation membrane system in living rat megakaryocytes. *Biophys. J.* 84:2646–2654.

Mason, M. J., and S. Grinstein. 1990. Effect of cytoplasmic acidification on the membrane potential of T-lymphocytes: Role of trace metals. *J. Membr. Biol.* 116:139–148.

Mason, M. J., J. Limberis, and G. G. Schofield. 1999. Transitional changes in membrane potential and intracellular $[Ca^{2+}]$ in rat basophilic leukemia cells. *J. Membr. Biol.* 170:79–87.

Mason, M. J., J. F. Hussain, and M. P. Mahaut-Smith. 2000. A novel role for membrane potential in the modulation of intracellular Ca^{2+} oscillations in rat megakaryocytes. *J. Physiol.* 524:437–446.

McCloskey, M. A., and M. D. Cahalan. 1990. G protein control of potassium channel activity in a mast cell line. *J. Gen. Physiol.* 95:205–227.

McCloskey, M. A., and Y. X. Qian. 1994. Selective expression of potassium channels during mast cell differentiation. *J. Biol. Chem.* 269: 14813–14819.

Montecucco, C., T. Pozzan, and T. Rink. 1979. Dicarbocyanine fluorescent probes of membrane potential block lymphocyte capping, deplete cellular ATP and inhibit respiration of isolated mitochondria. *Biochim. Biophys. Acta.* 552:552–557.

Mukai, M., I. Kyogoku, and M. Kuno. 1992. Calcium-dependent inactivation of inwardly rectifying K^+ channel in a tumor mast cell line. *Am. J. Physiol.* 262:C84–C90.

Neher, E., and B. Sakmann. 1978. The extracellular patch clamp: a method for resolving currents through individual open channels in biological membranes. *Pflugers Arch.* 375:219–228.

Orbach, H. S., L. B. Cohen, and A. Grinvald. 1985. Optical mapping of electrical activity in rat somatosensory and visual cortex. *J. Neurosci.* 5:1886–1895.

Pusch, M., and E. Neher. 1988. Rates of diffusional exchange between small cells and a measuring patch pipette. *Pflugers Arch.* 411:204–211.

Rae, J., K. Cooper, P. Gates, and M. Watsky. 1991. Low access resistance perforated patch recordings using amphotericin B. *J. Neurosci. Methods.* 37:15–26.

Rink, T. J., C. Montecucco, T. R. Hesketh, and R. T. Tsien. 1980. Lymphocyte membrane potential assessed with fluorescent probes. *Biochim. Biophys. Acta.* 595:15–30.

Rohr, S., and B. M. Salzberg. 1994. Characterization of impulse propagation at the microscope level across geometrically defined expansions of excitable tissue: multiple site optical recording of

transmembrane voltage (MSORTV) in patterned growth heart cell cultures. *J. Gen. Physiol.* 104:287–309.

Schofield, G. G., and M. J. Mason. 1996. A Ca^{2+} current activated by release of intracellular Ca^{2+} stores in rat basophilic leukemia cells (RBL-1). *J. Membr. Biol.* 153:217–231.

Simons, T. J. 1979. Actions of carbocyanine dyes on the Ca^{2+}-dependent K^+ channel in human red cell ghosts. *J. Physiol.* 288:481–507.

Somasundaram, B., and M. P. Mahaut-Smith. 1995. A novel monovalent cation channel activated by inositol trisphosphate in the plasma membrane of the rat megakaryocyte. *J. Biol. Chem.* 270:16638–16644.

Uneyama, C., H. Uneyama, and N. Akaike. 1993a. Cytoplasmic Ca^{2+} oscillations in rat megakaryocytes evoked by a novel type of purinoceptor. *J. Physiol.* 470:731–749.

Uneyama, H., C. Uneyama, and N. Akaike. 1993b. Intracellular mechanisms of cytoplasmic Ca^{2+} oscillations in rat megakaryocytes. *J. Biol. Chem.* 268:168–174.

Verheugen, J. A. H., H. P. M. Vijverberg, M. Oortgiesen, and M. D. Cahalan. 1995. Voltage-gated and Ca^{2+}-activated K^+ channels in intact human T lymphocytes. *J. Gen. Physiol.* 105:765–794.

Waggoner, A. S. 1979. Dye indicators of membrane potential. *Annu. Rev. Biophys. Bioeng.* 8:47–68.

Yamada, E. 1957. The fine structure of the megakaryocyte in the mouse spleen. *Acta Anat. (Basel).* 29:267–290.

Zhang, J., R. M. Davidson, M. D. Wei, and L. M. Loew. 1998. Membrane electric properties by combined patch clamp and fluorescence ratio imaging in single neurons. *Biophys. J.* 74:48–52.